

CAR⁺TCR-T cells co-expressing CD33-CAR and dNPM1-TCR as superior dual-targeting approach for AML treatment

Karin Teppert,^{1,5} Isabella Elias Yonezawa Ogusuku,^{1,5} Caroline Brandes,¹ Vera Herbel,¹ Nora Winter,¹ Niels Werchau,¹ Svetlana Khorkova,¹ Christian Wöhle,¹ Nojan Jelveh,¹ Kevin Bisdorf,¹ Boris Engels,¹ Thomas Schaser,¹ Kathleen Anders,^{2,4} Annette Künkele,^{2,3,4,6} and Dominik Lock^{1,6}

¹Miltenyi Biotec B.V. & Co. KG, 51429 Bergisch Gladbach, Germany; ²Department of Pediatric Oncology and Hematology, Charité-Universitätsmedizin Berlin, Corporate Member of Freie Universität Berlin, Humboldt-Universität zu Berlin, and Berlin Institute of Health, 10178 Berlin, Germany; ³German Cancer Consortium (DKTK), 10117 Berlin, Germany; ⁴German Cancer Research Center (DKFZ), 69120 Heidelberg, Germany

Acute myeloid leukemia (AML), a fast-progressing hematological malignancy affecting myeloid cells, is typically treated with chemotherapy or hematopoietic stem cell transplantation. However, approximately half of the patients face relapses and 5-year survival rates are poor. With the goal to facilitate dual-specificity, boosting anti-tumor activity, and minimizing the risk for antigen escape, this study focused on combining chimeric antigen receptor (CAR) and T cell receptor (TCR) technologies. CAR⁺TCR-T cells, co-expressing a CD33-CAR and a transgenic dNPM1-TCR, revealed increased and prolonged anti-tumor activity *in vitro*, particularly in case of low target antigen expression. The distinct transcriptomic profile suggested enhanced formation of immunological synapses, activation, and signaling. Complete elimination of AML xenografts *in vivo* was only achieved with a cell product containing CAR⁺TCR-T, CAR-T, and TCR-T cells, representing the outcome of co-transduction with two lentiviral vectors encoding either CAR or TCR. A mixture of CAR-T and TCR-T cells, without CAR⁺TCR-T cells, did not prevent progressive tumor outgrowth and was comparable to treatment with CAR-T and TCR-T cells individually. Overall, our data underscore the efficacy of co-expressing CAR and transgenic TCR in one T cell, and might open a novel therapeutic avenue not only for AML but also other malignancies.

INTRODUCTION

Acute myeloid leukemia (AML), a hematological malignancy originating from the myeloid lineage, poses significant challenges in treatment. The current standard of care primarily involves chemotherapy, which is optionally supplemented with hematopoietic stem cell transplantation as a consolidation therapy. However, response rates to this approach are often poor, with only 15% of the elderly and half of the under 60-year-old patients reaching 5-year survival, demonstrating the urgent need for better therapeutic alternatives.^{1,2} While effective in some cases, allogeneic hematopoietic stem cell transplantation carries the risk of lethal graft-versus-host toxicities.^{3,4} The recent

emergence of novel immunotherapies has fueled hope for better outcomes in AML treatment. For instance, the combination of chemotherapy with immunotherapies targeting checkpoint molecules or leukemia-associated antigens has led to first encouraging clinical results.^{2,5} However, their effectiveness in AML remains impaired, mainly due to the inherent challenges imposed by the broad clonal heterogeneity, the lack of leukemia-specific target antigens, and the highly immunosuppressive tumor microenvironment.^{6,7}

Adoptive cell therapies, particularly chimeric antigen receptor (CAR) T cell therapy, has achieved remarkable responses against other hematological malignancies. In AML, the antigens most frequently targeted by CAR therapy include CD33, CD123, or C-type lectin 1 (CLL1).⁷ These antigens are also found on non-malignant, healthy cells. CD33 is for example expressed on myeloid progenitors, immune cells, and hepatic Kupffer cells, which poses an increased risk for on-target off-tumor toxicity and severe side effects.⁷⁻⁹ Similarly, CD123 targeting may lead to capillary leakage syndrome due to on-target off-tumor toxicity against endothelial cells.¹⁰ The genetic and phenotypic diversity of AML poses another considerable challenge, promoting not only the outgrowth of chemotherapy-resistant leukemic clones, but also the escape of antigen-negative blasts, leading to disease recurrence after targeted immunotherapy.^{11,12} Thus, several clinical CAR-T cell trials have adopted combinatorial strategies targeting two different antigens simultaneously (NCT05016063,¹³ NCT04156256,¹⁴ or NCT03631576¹⁵).

Transgenic T cell receptors (TCRs) have been suggested as a highly leukemia-specific alternative, reducing the risk for on-target

Received 7 January 2024; accepted 20 March 2024;
<https://doi.org/10.1016/j.omton.2024.200797>.

⁵These authors contributed equally

⁶These authors contributed equally

Correspondence: Dominik Lock, PhD, Miltenyi Biotec B.V. & Co. KG, 51429 Bergisch Gladbach, Germany.

E-mail: dominiklo@miltenyi.com



off-tumor effects when targeting intracellularly processed antigens, and particularly specific, tumor-derived neoantigens.^{7,16} Neoantigens are newly formed antigens that arise from mutations within tumor cells, distinguishing them from normal cells and serving as potential targets for immunotherapy.¹⁷ In the context of AML, approximately 30% of cases display a driver mutation in exon 12 of nucleophosmin 1 (NPM1).^{18,19} Van der Lee and colleagues have identified an HLA-A2*02:01-restricted dNPM1-TCR, specific for the neo-epitope CLAVEEVSL and demonstrated reactivity against primary AML cells both *in vitro* and *in vivo*.¹⁹

To advance the treatment of AML, the goal of this study was to join the potential of CAR and TCR technologies, as previously proposed.²⁰ We engineered CAR⁺TCR-T cells, co-expressing the recently identified dNPM1-TCR and a second-generation CD33-CAR incorporating an scFv derived from clone My96.^{19,21,22} This approach was designed to counteract several of the aforementioned challenges: First, targeting of a neoantigen such as dNPM1 was envisioned to minimize the risk for on-target off-tumor toxicities due to the high specificity for leukemic blasts.¹⁶ Second, by simultaneous targeting of dNPM1 and the leukemia-associated antigen CD33, we aimed to mitigate the risk for tumor escape and relapse.¹³ Finally, we analyzed whether CAR⁺TCR-T cells demonstrate boosted anti-tumor cytotoxicity, due to benefiting from signaling through both TCR and CAR.

RESULTS

CAR⁺TCR-T cells demonstrated increased cytotoxicity upon dual stimulation

With the goal to facilitate dual-specificity, boosting anti-tumor activity, and minimizing the risk for antigen escape, we engineered CAR⁺TCR-T cells co-expressing a CAR and a transgenic TCR targeting AML. CAR⁺TCR-T cells were produced through co-transduction of CD8⁺ T cells using two lentiviral vectors encoding for either CD33-CAR or dNPM1-TCR (Figure 1A). As expected, the frequency of double-positive T cells after co-transduction was generally lower than the proportion of CAR- or TCR-expressing cells after transduction with only one lentiviral vector (Figure 1B). To facilitate comparable and high expression levels of above 80%, all effector cell types were sorted via CD33-CAR and/or dNPM1-TCR prior to *in vitro* co-culture assay (Figure 1C). Moreover, the mean fluorescent intensities (MFIs) were determined, indicating comparable CAR and TCR expression levels between CAR only, TCR only, and CAR⁺TCR-T cells (Figure 1D).

To evaluate the functionality of CAR⁺TCR-T cells under single and dual stimulation conditions and compare it with T cells expressing only CAR or TCR, various co-culture scenarios were designed (Figure 1E). The experimental setup allowed for controlled stimulation of CAR or TCR, or both (dual stimulation) by utilizing various OCI-AML cell lines expressing either only CAR- or TCR-target, or both, respectively. Dual stimulation was either achieved in *cis* or in *trans*, meaning expression of dNPM1 or CD33 on the same or on different target cell lines, respectively. The *trans* setting allowed for discrimination between TCR- and CAR-dependent target cell lysis by CAR⁺TCR-T cells. The goal of this study was not only to examine

the functionality of CAR⁺TCR-T compared with CAR-T or TCR-T cells, but also compared with the alternative dual-targeting approach called Double-T, involving a mixture of CAR-T and TCR-T cells. Moreover, as sorting of T cells is not feasible for clinical application, we also implemented a third dual-targeting strategy, called Triple-T, which mimics the natural product of co-transduction, encompassing CAR-T, TCR-T, and CAR⁺TCR-T in equal proportions. No significant difference was observed between CAR⁺TCR-T or single-transduced T cells upon stimulation of only TCR or CAR (Figure 1F). Dual stimulation in *trans* resulted in significantly enhanced lysis of the TCR-target cell line. This cytotoxic boost in *trans* was not observed comparing CAR⁺TCR-Ts with scenarios involving CAR-Ts: In all conditions involving CAR⁺ cells (CAR-T, CAR⁺TCR-T, Double-T and Triple-T), CAR-target cell lysis was nearly complete in the *trans* setting. In the *cis* setting, however, CAR⁺TCR-T cells outperformed not only TCR-T cells but also exhibited superior performance compared with CAR-T cells. Since CAR-T cell efficacy depends on the target antigen level, we screened our target cell lines for CD33 expression. OCI-AML3 cells used for *cis* stimulation showed 4-fold lower expression of the CAR target antigen CD33 than the OCI-AML2 cell line, which was used for stimulation via CAR (Figure S1A). As expected, the CD33 expression level influenced CAR functionality (Figure S1B), explaining the discrepancy in the CAR-mediated cytotoxic potential comparing the *trans* and the *cis* setting using various target cell lines. While CAR⁺TCR-T cells outperformed CAR-T or TCR-T cells upon dual stimulation, no significant difference was observed compared with the other dual-targeting approaches Double-T and Triple-T. To ensure equivalent total cell counts across all effector cell conditions, and simultaneously, comparable numbers of CAR- and TCR-expressing T cells, CAR⁺TCR-T composed a 1:1 mixture of CAR⁺/TCR⁺ double-positive T cells and UTD-T cells. Double-T, on the other hand, contained a 1:1 mixture of CAR-T and TCR-T, and consequently, twice as many engineered effector cells as CAR⁺TCR-T. Despite this numerical difference, CAR⁺TCR-T cells and Double-T cells led to comparable target cell lysis in *cis* and in *trans*.

In summary, CAR⁺TCR-T cells were produced through co-transduction of CD8⁺ T cells using two lentiviral vectors encoding for either CD33-CAR or dNPM1-TCR. Compared with CD33-CAR-T cells or dNPM1-TCR-T cells, CAR⁺TCR-T cells demonstrated similar cytotoxicity upon stimulation of only CAR or only TCR, respectively. However, dual stimulation of both CAR and TCR led to significantly enhanced target cell lysis by CAR⁺TCR-T cells, especially against low CAR antigen-expressing target cells.

Sustained superiority of CAR⁺TCR-T cells after repetitive stimulation

To explore whether simultaneous stimulation through CAR and TCR results in faster exhaustion of CAR⁺TCR-T cells, we performed long-term repetitive co-culture experiments. Confirming our earlier finding from short-term stimulation, CAR⁺TCR-T cells continued to outperform CAR-T and TCR-T cells in the *trans* setting (different target antigens on different tumor cells), even after repetitive antigen

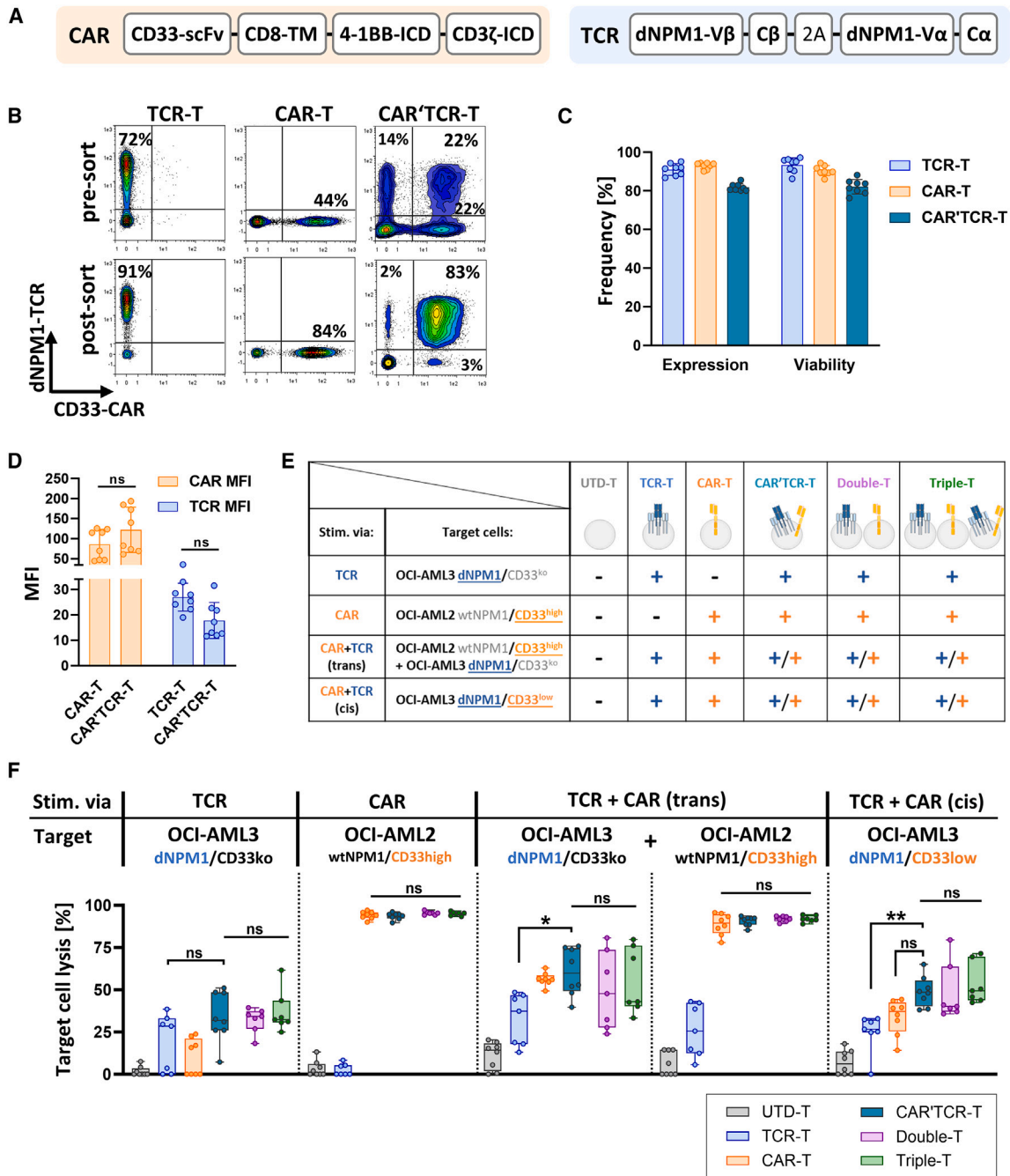


Figure 1. Functional superiority of CAR+TCR-T cells co-expressing CD33-CAR and dNPM1-TCR

CAR+TCR-T cells were manufactured through co-transduction with two lentiviral vectors encoding for CD33-CAR or dNPM1-TCR. (A) Schematics of the CD33-CAR containing a CD33-targeting single-chain variable fragment (scFv), a CD8 transmembrane domain (TM), 4-1BB and CD3ζ intracellular domains (ICD), and of the dNPM1-TCR containing dNPM1-specific variable alpha and beta chains (Vα and Vβ) as well as the respective constant chains (Cα and Cβ). (B) Representative dot plots displaying CAR and TCR expression pre- and post-sorting. (C) Viability and percentage of CAR+, TCR+, or double-positive T cells and (D) mean fluorescence intensity (MFI) of CAR or TCR prior to *in vitro* co-culture experiment. (E) Experimental setup illustrating various effector cell conditions and controlled stimulation via CAR, TCR, or both through co-culture with different target cell lines. Double-T consisted of a mixture of CAR-T and TCR-T cells and Triple-T of CAR+TCR-T, CAR-T, and TCR-T. *Trans*: stimulation via target cells expressing both CD33 and dNPM1; *Cis*: stimulation via a mixture of target cells expressing either CD33 or dNPM1. (F) Target cell lysis after 18 h of co-culture at an E:T ratio of 1:1. Displayed are individual and median values (±IQR) of eight different donors from two independent experiments. The *p* values (ns, not significant; **p* ≤ 0.05, ***p* ≤ 0.01) were determined using ordinary one-way ANOVA with Tukey's correction.

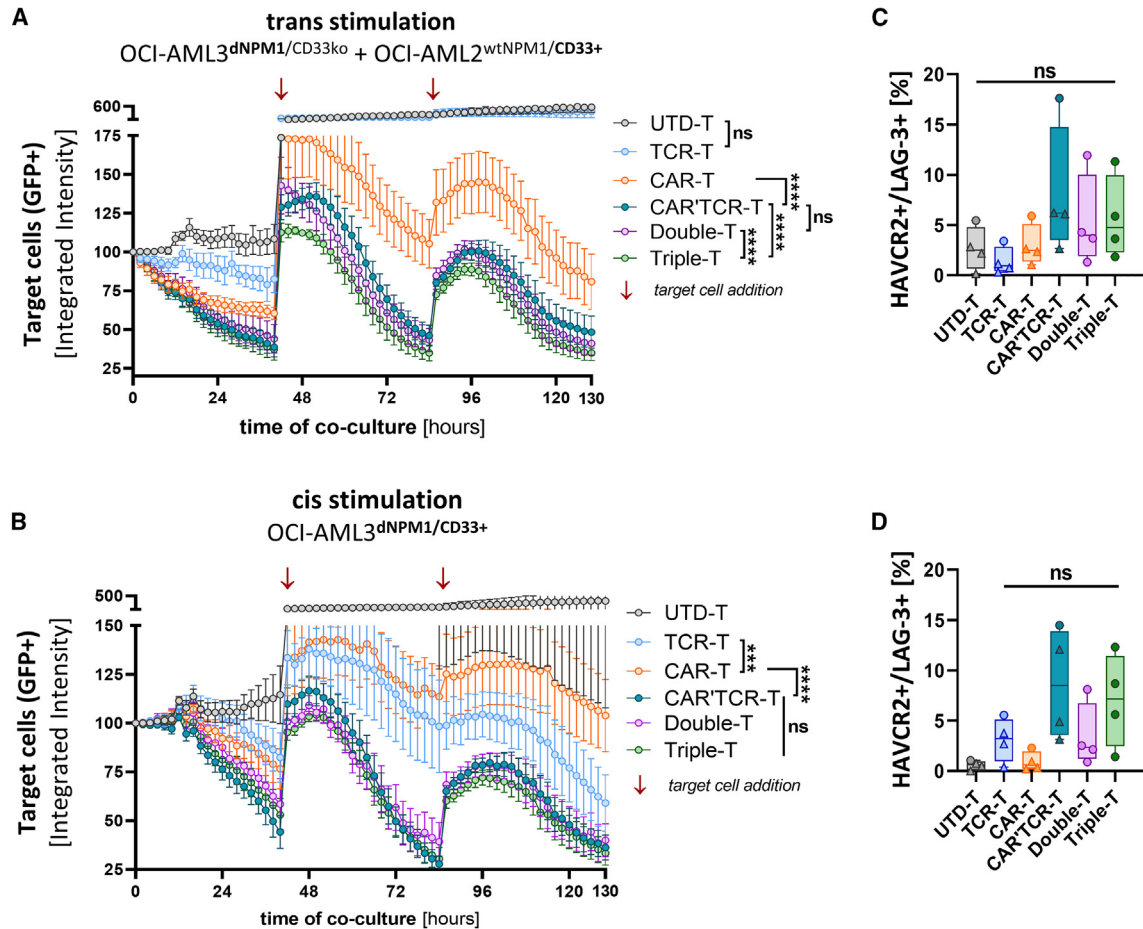


Figure 2. CAR⁺TCR-Ts showed significantly prolonged target cell lysis upon repetitive stimulation

Live-cell imaging of long-term repetitive co-culture with UTD-T, TCR-T, CAR-T, CAR⁺TCR-T cells, Double-T (mixture of CAR-T and TCR-T cells), and Triple-T (mixture of CAR-T, TCR-T, and CAR⁺TCR-T cells). Stimulation was facilitated (A) in *trans* (CAR- and TCR-target on different cells) and (B) in *cis* (CAR- and TCR-target on same cell line). Red arrows indicate the addition of new target cells to the co-culture. Displayed are mean values (\pm SEM) of eight different donors from two independent experiments. The *p* values (ns, not significant; **p* \leq 0.05, ***p* \leq 0.01, ****p* \leq 0.001) were determined using Tukey's multiple comparison test with mixed-effects model and Geisser-Greenhouse correction (two-way ANOVA). Proportion of HAVCR2⁺/LAG-3⁺ cells in different effector cell conditions after 130 h of co-culture in (C) *trans* and (D) *cis*. Displayed are individual and median values (\pm IQR) for four different donors. The *p* values (ns, not significant; **p* \leq 0.05) were calculated using ordinary one-way ANOVA with Tukey's correction for multiple comparison.

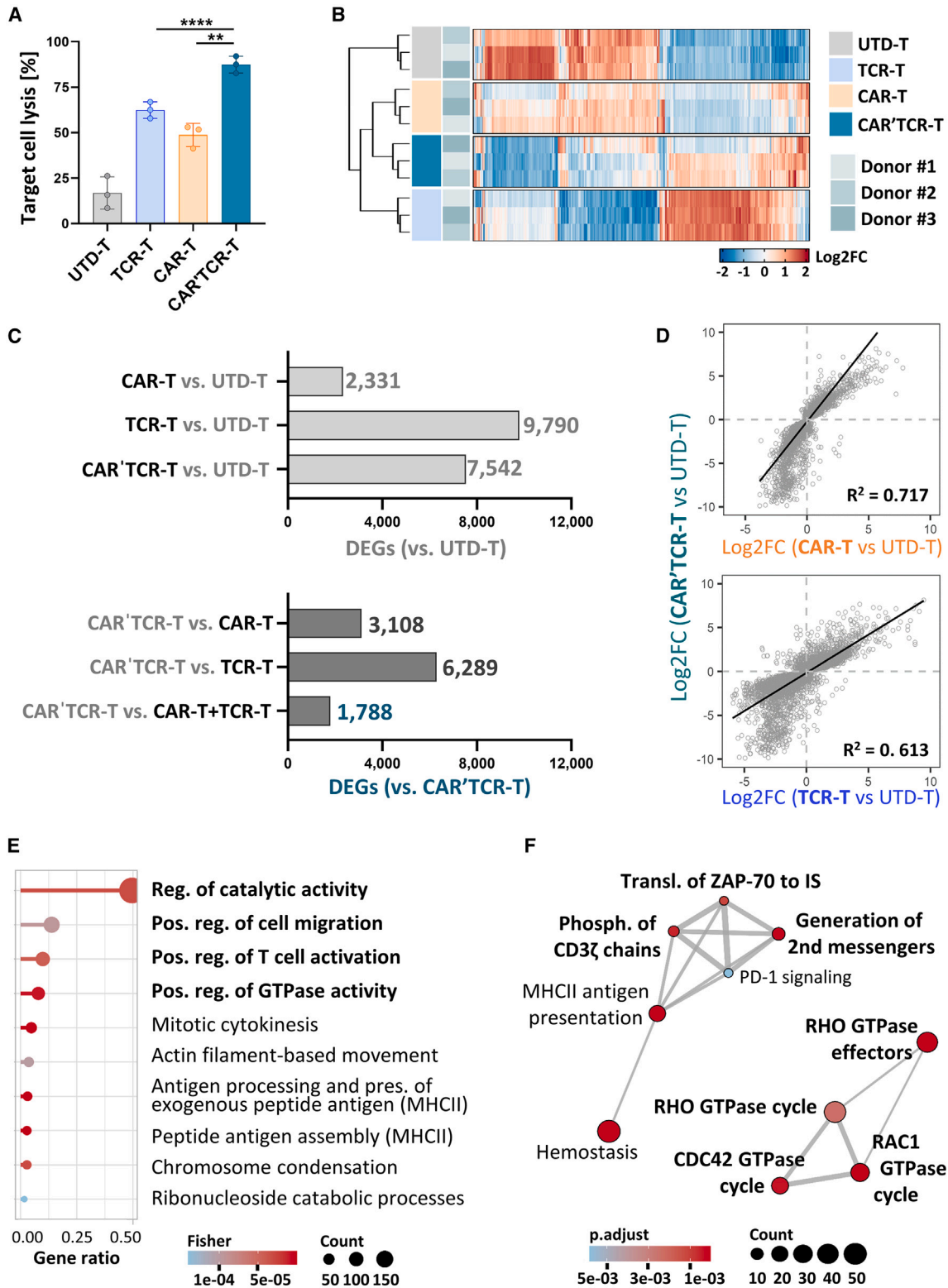
exposure (Figure 2A). This ability to kill TCR-target negative cells via the CAR or CAR-target negative cells via the TCR underscores their potential advantage in addressing clonal heterogeneity, which represents a major challenge in treatment of AML. Furthermore, CAR⁺TCR-T cells displayed significantly stronger cytotoxicity than CAR-T or TCR-T after repeated engagement with target cells in *cis* configuration, where the target cell line expressed both CD33 and dNPM1 (Figure 2B). Consistent results were obtained comparing CAR⁺TCR-T, Double-T, and Triple-T, all facilitating potent target elimination throughout the third round of stimulation.

After 130 h of co-culture and three rounds of repetitive tumor cell challenge, we assessed effector cell exhaustion by evaluating the expression of exhaustion markers HAVCR2 (formerly known as

TIM-3) and LAG-3 (Figures 2C and 2D). Although statistically not significant, CAR⁺TCR-T cells displayed a slightly higher proportion of HAVCR2⁺/LAG-3⁺ T cells, particularly compared with Double-T cells. This trend could potentially suggest a tendency of accelerated exhaustion in T cells exposed to dual stimulation. However, further analysis is required to draw a reliable conclusion. Overall, CAR⁺TCR-T cells demonstrated sustained cytotoxicity upon repetitive target cell encounter and superiority compared with CAR-T or TCR-T cells.

CAR⁺TCR-T displayed a unique transcriptomic gene profile

Whole transcriptome analysis of CAR⁺TCR-T, CAR-T, TCR-T, and UTD-T cells was performed after an 18 hours *cis* stimulation with CD33⁺ dNPM1⁺ OCI-AML3 target cells. Our primary objective



(legend on next page)

was to identify unique characteristics in the transcriptomic profile of CAR⁺TCR-T cells, especially compared with CAR-T or TCR-T cells. Consistent with previous results, CAR⁺TCR-T cells showed significantly increased target cell lysis compared with T cells expressing either CAR or TCR (Figure 3A). To ensure high purity of effector cells for RNA sequencing (RNA-seq), target cells were magnetically depleted using CD4- and CD15-specific beads after co-culture. As expected, the various effector cell types grouped into separated hierarchical clusters. Among the 500 most variable genes, CAR⁺TCR-T cells demonstrated an RNA-seq profile suggesting higher similarity compared with CAR-T than TCR-T cells (Figure 3B). In the following, differential gene expression analysis was performed. In reference to UTD-T cells, TCR-T cells yielded the largest number of differentially expressed genes (DEGs), in total 9,790 compared with UTD-T cells (Figure 3C). CAR⁺TCR-T cells and CAR-T cells displayed 7,542 and 2,331 DEGs compared with UTD-T, respectively. To determine similarities in the regulation of CAR⁺TCR-T cells and CAR-T or TCR-T cells, we compared the resulting Log₂ fold changes of each analysis specifically for the subset of 7,542 genes that were found to be differentially expressed in CAR⁺TCR-T (Figure 3D). Intriguingly, linear regression analysis demonstrated a stronger relationship between CAR⁺TCR-T cells and CAR-T cells (71%) than between CAR⁺TCR-T cells and TCR-T cells (61%). This observation suggests that CAR signaling exerts a more dominant influence in CAR⁺TCR-T cells compared with TCR signaling.

Besides determining the similarities, it was important to address the question of whether CAR⁺TCR-T cells display a unique RNA-seq profile. To address this, gene set enrichment analysis was performed using the 1,788 DEGs in CAR⁺TCR-T cells compared with both CAR-T and TCR-T cells (Figure 3C). TopGO and Reactome databases were applied for functional annotation in separate analysis for up- (865) and downregulated (924) genes in CAR⁺TCR-T cells.^{23–25} CAR⁺TCR-T cells primarily demonstrated enrichment for TopGO gene ontology terms such as regulation of catalytic activity, positive regulation of T cell activation, migration, and GTPase activity (Figure 3E). Consistent with this, analysis using Reactome database identified cellular pathways relating to RHO GTPase effectors and cycles, including the GTPase cell division cycle protein 42 (CDC42) and Rac family small GTPase 1 (RAC1) (Figure 3F). This strongly suggests increased T cell activation, signaling, and immunological synapse formation, since both CDC42 and RAC1 play crucial roles in cytoskeletal reorganization, activation-dependent lipid raft formation, T cell polarization, and migration.^{26,27} As expected, the opposite was observed upon gene set enrichment analysis of the DEGs significantly downregulated in CAR⁺TCR-T cells. The gene ontology category “negative

downregulation of signal transduction” was most enriched and significant in DEGs downregulated in CAR⁺TCR-T cells (Figure S2A). The functional annotation of upregulated DEGs using the Reactome database also displayed pathways corresponding to CD3 ζ chain phosphorylation, ZAP-70 translocation to the immunological synapse, and generation of second messenger molecules. This further verified the analysis with TopGO, and overall, the increased cytotoxic potential of CAR⁺TCR-T cells. Analysis with Reactome for the DEGs downregulated in CAR⁺TCR-T cells primarily displayed G protein-coupled receptor pathways including G α (i) signaling (Figure S2B).

Overall, CAR⁺TCR-T cells displayed a mixed gene expression profile that is more similar to CAR-T than TCR-T cells, indicative for CAR signaling being more dominant than TCR signaling. Most importantly, CAR⁺TCR-T cells demonstrated a unique set of DEGs in comparison with CAR-T or TCR-T cells.

Enhanced *in vivo* efficacy of CAR⁺TCR-T cells in a mouse model with human AML xenograft

With the goal to assess the efficacy of CAR⁺TCR-T cells in an AML mouse model, NSG mice were intravenously injected with OCI-AML3 cells expressing the CAR- and TCR-targets (Figure 4A). Effector cells were manufactured using the fully closed and automated CliniMACS Prodigy and intravenously injected after 4 days of tumor engraftment. Given that Triple-T showed comparable *in vitro* anti-tumor activity compared with CAR⁺TCR-T (Figures 1 and 2) and sorting of cells is difficult to put into clinical practice, our *in vivo* study was based on Triple-T cells. This cell product was produced via co-transduction with two lentiviral vectors either encoding CD33-CAR or dNPM1-TCR, resulting in a composition of CAR⁺TCR-T as well as CAR-T, TCR-T cells. Normalization of the various effector cell conditions was performed prior to injection to ensure comparable transduction efficiencies of approximately 60% (Figure 4B).

After randomization, comparable tumor burden was observed between the several treatment groups (Figure 4C). During the first 23 days of the *in vivo* study, all treatment groups exhibited progressive OCI-AML3 growth, as evidenced by an increase of luminescence signal produced by the firefly luciferase-transgenic tumor cells (Figures 4D and 4E). Strikingly, only mice treated with Triple-T demonstrated tumor reduction starting from day 28, resulting in reduction of the light signal by two logarithmic units in five out of eight mice (Figure 4E). All other groups reached study endpoint criteria by day 37 and had to be removed from the experiment (Figure 4F). Repetition of the *in vivo* study with T cells from another donor led to the same result and proved the reliability of the

Figure 3. CAR⁺TCR-T cells show RNA-seq profile linked to enhanced T cell activation and signaling

(A) Target cell lysis after 18 h of co-culture with OCI-AML3 (*cis* stimulation) at an E:T ratio of 2:1. Displayed are individual and mean values (\pm SD) of three different donors. The p values ($*p \leq 0.05$, $**p \leq 0.01$, $***p \leq 0.001$, $****p \leq 0.0001$) were determined using ordinary one-way ANOVA with Tukey's correction. (B) Hierarchical clustering of 500 most variable genes among UTD-T, CAR-T, TCR-T, and CAR⁺TCR-T cells. Gene expression was scaled to have mean equal zero. (C) DEGs identified from comparison with UTD-T or with CAR⁺TCR-T cells displayed in the upper and lower graph, respectively. (D) Log₂ fold changes of 7,542 DEGs from CAR⁺TCR-T vs. UTD-T were compared with Log₂ fold changes in CAR-T vs. UTD-T (upper graph) or TCR-T vs. UTD-T (lower graph). Linear regression was determined using R². Gene set enrichment analysis showing 10 most significant (E) TopGO gene ontology terms and (F) Reactome pathways of upregulated DEGs (864) in CAR⁺TCR-T cells compared with CAR-T and TCR-T cells.

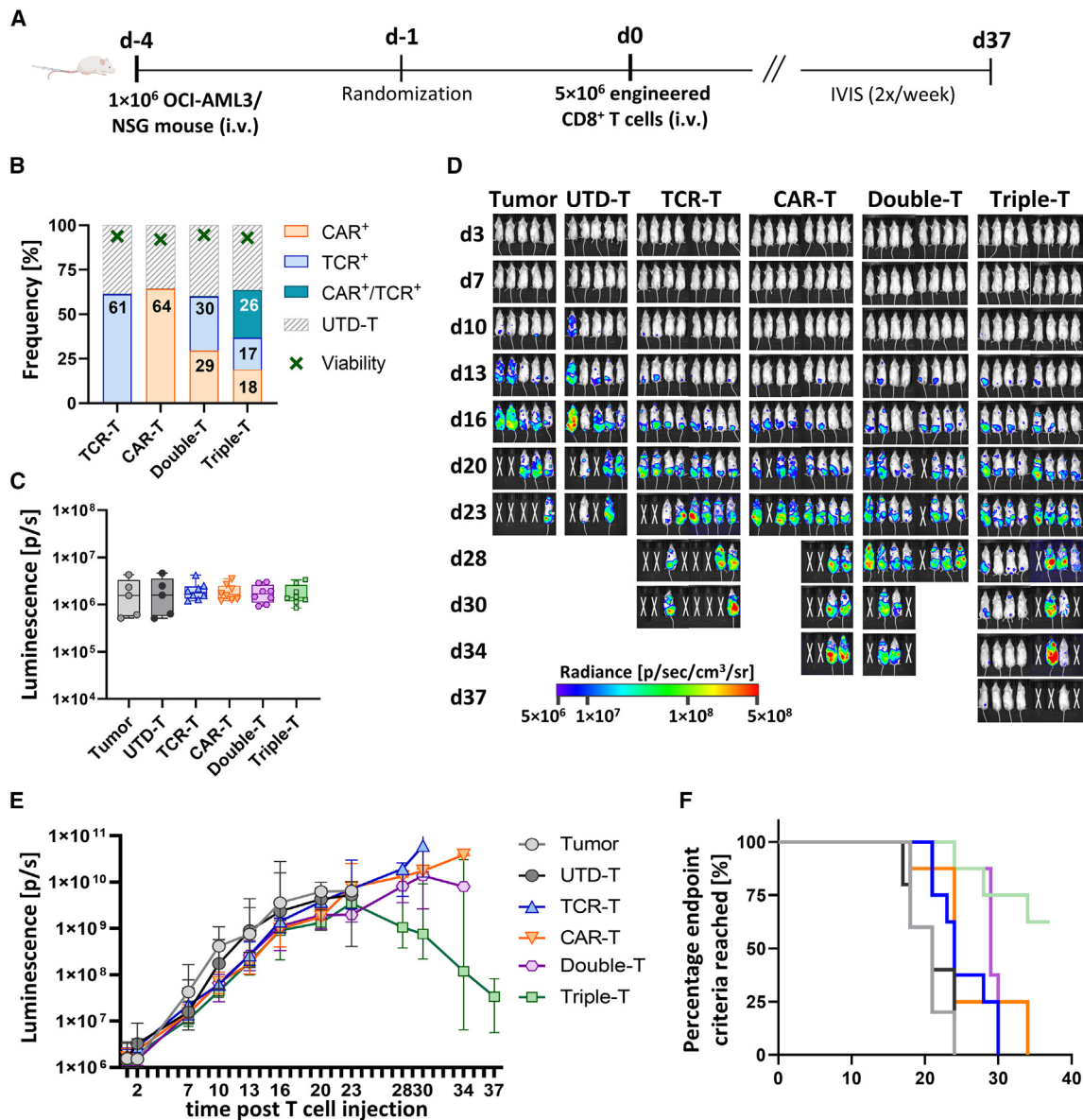


Figure 4. Tumor elimination *in vivo* only achieved with CAR⁺TCR-T-containing Triple-T

(A) Schematic representation of the *in vivo* efficacy study plan using NSG mice bearing human AML tumor xenografts. (B) Percentages of CAR⁺ and/or TCR⁺ T cells in various treatment conditions: TCR-T cells, CAR-T cells, Double-T (mixture of CAR-T and TCR-T cells), and Triple-T (mixture of CAR-T, TCR-T, and CAR⁺TCR-T cells). Frequency of viable cells is indicated by a green x. (C) Randomization of mice according to tumor size 3 days after tumor cell injection. All groups consisted of eight mice, except tumor only and untransduced (UTD-T) with five mice per group. Displayed are individual and median values (\pm IQR). (D) Bioluminescence images and (E) plotted median values with interquartile range were measured twice a week over the course of in total 37 days. (F) Percentage of mice that reached study endpoint criteria and needed to be removed from the experiment.

findings (Figure S3). In contrast to the *in vitro* findings, Triple-T not only outperformed CAR-T and TCR-T, but also demonstrated superior efficacy compared with Double-T cells. This suggests that under such challenging conditions, CAR⁺TCR-T cells co-expressing CAR and TCR are required to achieve a sufficient anti-tumor response, unattainable by the mere mixture of CAR-T and TCR-T cells.

Since Triple-T comprised CAR⁺TCR-T, CAR-T, and TCR-T, it was crucial to dissect which of these effector cell types demonstrated the longest persistence. Interestingly, *ex vivo* analysis of spleens isolated from treated mice after 37 days showed that the majority of the remaining cells were CAR⁺ T cells. Prior to injection, Triple-T consisted of 18% CAR-T, 17% TCR-T, and 26% CAR⁺TCR-T cells. Post-experiment analysis displayed shifted

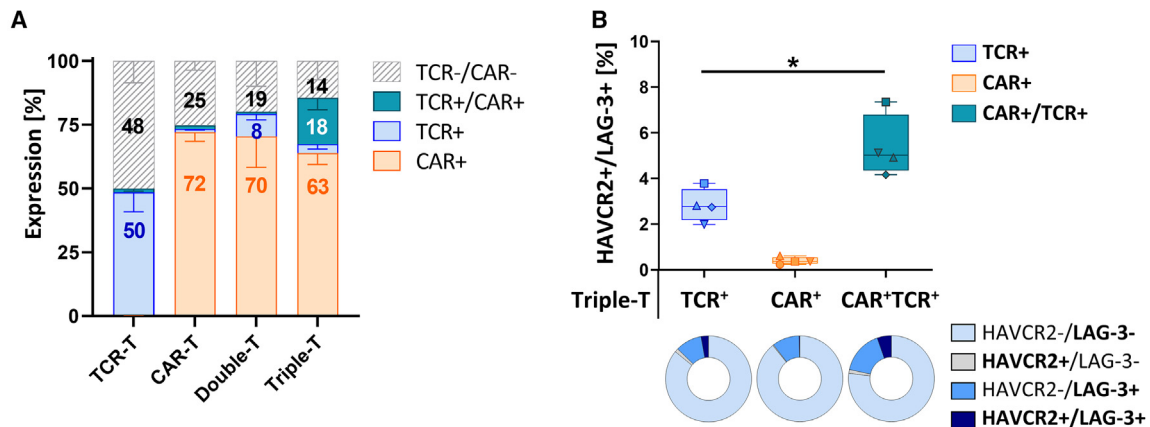


Figure 5. Ex vivo-analyzed CAR-T cells show higher persistence and reduced exhaustion compared with CAR⁺TCR-T

(A) *Ex vivo* spleen analysis displaying the frequencies of effector subtypes, meaning untransduced, CAR⁺, TCR⁺, or double-positive T cells, in the various treatment conditions. Displayed are mean values (\pm SD) for six mice per group. (B) Proportions of HAVCR2-/LAG-3-expressing TCR⁺, CAR⁺ or double-positive cells in Triple-T at study endpoint (d37). Bar graphs display distribution of HAVCR2-and/or LAG-3-expression in different subtypes. Displayed are individual and median values (\pm IQR) for four Triple-T-treated mice. The *p* value ($*p \leq 0.05$) was determined via Holm-Sidak's multiple comparison test (one-way ANOVA) with mixed-effects model and Geisser-Greenhouse correction.

frequencies with 63% CAR-T, 4% TCR-T, and 18% CAR⁺TCR-T (Figure 5A). The fact that tumor elimination was only achieved with Triple-T, while tumors treated with Double-T progressively grew, evidenced the necessity for including CAR⁺TCR-T cells. However, due to the lower persistence of CAR⁺TCR-T cells compared with CAR-T cells, it was hypothesized that this was linked to higher exhaustion of CAR⁺TCR-T cells. Indeed, *ex vivo* exhaustion marker analysis of the various subpopulations in Triple-T demonstrated significantly increased expression of HAVCR2 and LAG-3 in CAR⁺TCR-T cells, especially compared with CAR-T cells (Figure 5B). However, the frequency of HAVCR2⁺/LAG-3⁺ T cells remained relatively low, comprising less than 8% of the population. Notably, the prevailing proportion consisted of cells devoid of exhaustion markers, with 76% and 89% of the cells being double-negative for HAVCR2⁻ and LAG-3⁻ in CAR⁺TCR-T and CAR-T, respectively. Thus the shift in frequencies, from 18% of CAR-T cells within the administered Triple-T cell product to 63% of CAR-T cells within the cells analyzed *ex vivo*, is more likely attributed to a proliferative advantage exhibited by CAR-T cells rather than the exhaustion of CAR⁺TCR-T cells. In summary, *ex vivo* analysis of the three T cell subpopulations in Triple-T revealed higher exhaustion marker expression in CAR⁺TCR-T cells and lower persistence compared with CAR-T cells but not TCR-T cells.

In closing, Triple-T demonstrates the natural product of co-transduction with two different lentiviral vectors and was the only condition that led to tumor elimination *in vivo*. Even treatment with dual-targeting Double-T cells, consisting of CAR-T and TCR-T, resulted in persistent proliferation of target cells, further underlining the boosted anti-tumor response with CAR⁺TCR-T cells.

DISCUSSION

Our primary goal was to assess whether it is advantageous to combine CAR and TCR technologies for the treatment of AML. Due to the broad clonal heterogeneity in AML, several multi-targeting approaches have been introduced and are currently being tested.¹¹⁻¹⁵ In this work, special focus was put on the side-by-side comparison of CAR⁺TCR-T cells, co-expressing a CAR and a transgenic TCR, and the dual-targeting alternative of mixing CAR-T cells with TCR-T cells (referred to as Double-T). Our data showed that concomitant signaling in CAR⁺TCR-T cells via CD33-CAR and dNPM1-TCR boosted the anti-tumor cytotoxicity, thereby outperforming CAR-T and TCR-T cells *in vitro* and *in vivo*.

CAR⁺TCR-T cells were generated by simultaneously co-transducing T cells with two lentiviral vectors, encoding for a second-generation 4-1BB-costimulated CD33-CAR (My96 clone-derived scFv^{8,21,28}) and a neoantigen-targeting dNPM1-TCR.^{19,22} Before studying the functionality of CAR⁺TCR-T cells upon dual stimulation, we addressed concerns of potential reciprocal inhibition arising from single stimulation via CD33-CAR or dNPM1-TCR only. Such inhibition could potentially impair functionality of CAR⁺TCR-T cells, particularly in scenarios where tumors exhibit heterogeneous target antigen expression. Our data demonstrated that stimulation of only CAR or only TCR resulted in comparable cytotoxicity between CAR⁺TCR-T cells or single-transduced T cells. Moreover, upon dual stimulation, CAR⁺TCR-T cells demonstrated functional superiority compared with CAR-T cells or TCR-T cells *in vitro* and *in vivo*. Enhanced cytotoxicity was not only observed upon dual stimulation in *cis* (CAR- and TCR-target on same cell line), but also in *trans* (CAR- and TCR-target on two different cell lines), which represents a potential benefit regarding the broad AML heterogeneity. The *in vivo* efficacy study clearly displayed the enhanced potency of CAR⁺TCR-T cells

to achieve tumor elimination: Only treatment with Triple-T, meaning the product of co-transduction composed of CAR-T, TCR-T, and CAR^TTCR-T, induced tumor reduction. Most importantly, Double-T cells (pooled CAR-T and TCR-T cells) led to continuous *in vivo* tumor outgrowth, indicating that dual-specificity is not the only solution and that the boosted anti-tumor response through CAR^TTCR-T cells facilitates the distinctive impact. Such increase in cytotoxicity might represent the needed optimization for treatment of AML to achieve powerful and complete tumor elimination.^{29,30}

Compared with CAR-T, TCR-T, or UTD-T cells, the distinct transcriptomic profile of CAR^TTCR-T cells strongly suggested synergistic effects through simultaneous signaling via CAR and TCR. Enrichment of gene ontology terms corresponding to positive regulation of T cell activation and GTPase activity as well as CDC42 and RAC1 GTPase cycles was strongly indicative of enhanced T cell activation, immunological synapse formation, and proximal signaling. Moreover, DEGs that were significantly downregulated in CAR^TTCR-T cells were primarily linked to “negative downregulation of signal transduction” and to G protein-coupled receptor pathways including Gα(i) signaling. The latter is a subunit of the heterotrimeric G-protein complex and plays a role in cell signaling pathways. It was described to be excluded from the immunological synapse upon TCR engagement, in order to shift chemokine receptor activities from migration to cell adhesion, thereby promoting TCR proximal signaling.^{31,32} In general, it is crucial to note that GPCRs regulate a wide variety of cellular mechanisms.^{33,34} Thus, conclusions regarding cellular mechanisms need to be drawn carefully. Consistent with the increased functionality *in vitro* and *in vivo*, CAR^TTCR-T cells demonstrated a distinct transcriptomic profile with significantly upregulated DEGs, involved in enhanced immunological synapse formation, T cell activation, and signaling.

Although a manufacturing process with co-transduction is clinically translatable, further studies need to be performed to assess whether the cellular composition in Triple-T is superior compared with a cell product solely consisting of CAR^TTCR-T cells. To achieve this, high-capacity viral vectors or implementation of novel gene-transfer technologies would be required to achieve sufficient transduction and expression levels.^{35,36} Interestingly, *ex vivo* analysis at study endpoint showed that Triple-T mainly consisted of CAR-T cells, suggesting that CAR^TTCR-T cells display reduced persistence. Continuous CD33-targeting in AML elevates the risk of myelosuppression or severe sinusoidal obstruction syndrome, attributed to on-target off-tumor toxicity against myeloid progenitors or Kupffer cells, respectively.^{9,37,38} Therefore, it might even be advantageous for AML treatment to have a high purity of CAR^TTCR-T cells, which initially provide a powerful and comprehensive cytotoxic response, but eventually, lower persistence and risk of chronic side effects than CAR-T cells. The implementation of innovative technologies may offer a pathway to mitigate myelotoxicities and enhance safety. One potential approach to achieve this could involve replacing the CD33-CAR with a CD33-targeting chimeric costimulatory receptor that lacks the CD3ζ signaling domain. Such “AND” logic gating has

already successfully been achieved for CD33-/CD123-and CD33-/HAVCR2-dual-targeting CAR-T cells.^{39,40} Even greater tumor cell specificity can be anticipated when combined with a neoantigen-targeting dNPM1-TCR. Alternative solutions to avoid prolonged myelosuppression might be the transient or inducible expression of the CD33-CAR.^{8,41} Myeloid development and function was shown to be independent of CD33, thus allowing for CD33 knockout from donor-derived hematopoietic stem cells without affecting hematopoiesis.^{42,43} In combination with CD33-CAR T cell infusion, this enables the elimination of leukemic cells while preserving non-malignant hematopoietic cells. Similarly, allogeneic CAR^TTCR-T cells could be combined with prior transplantation of CD33-deleted hematopoietic stem cells.

While working with neoantigen-specific transgenic TCRs ensures high tumor cell restriction, it automatically entails that the treatment is only applicable to a certain group of patients. CD33 is expressed in the majority of leukemic blasts, but the driver mutation dNPM1 is only found in approximately 30% of all AML patients.^{18,19} Although another dNPM1-TCR specific for HLA-A*11:01 has already been described,⁴⁴ further expansion of the available dNPM1-TCR selection is required to enable flexible therapy adjustments according to the patient’s HLA haplotype.

Finally, cell-based therapy was described to be diminished by the immunosuppressive AML niche, causing T cell exhaustion and reducing therapeutic efficiency.⁵ Therefore, several groups aimed at combining CAR-T cells with checkpoint inhibitors, which might also support the anti-leukemia effect of CAR^TTCR-T cells.^{7,8} Additionally, targeting of HAVCR2 or LAG-3 might help to minimize the slightly enhanced exhaustion observed in the CAR^TTCR-T cell subpopulation of Triple-T. To this end, studying CAR^TTCR-T cell functionality in a patient-derived xenograft mouse model would display a possible setting for testing such combinatorial strategies and to further verify our findings.⁴⁵

This work evidenced the therapeutic potential of CAR^TTCR-T cells, strongly supporting the approach of joining forces through combining a CAR and a transgenic TCR in the same T cell. Owing to the dual-specificity and the boosted cytotoxic potency, CAR^TTCR-T cells might display a possible approach, especially for chemotherapy-resistant AMLs. Moreover, it is important to highlight the superiority of CAR^TTCR-T cells in detecting and eliminating tumor cells expressing only low levels of CD33 target antigen. Together, this might support robust and thorough tumor clearance, thereby decreasing the risk for relapse due to residual target antigen-negative leukemic blasts.¹³ Especially the enhanced performance compared to a mixture of CAR-T and TCR-T cells, underlines the therapeutic power of CAR^TTCR-T cells, also for potential application in other tumor settings.

MATERIALS AND METHODS

Unless otherwise noted, all reagents and kits were from Miltenyi Biotec, Bergisch Gladbach, Germany.

Cell lines and culture conditions

HEK293T cells (DSMZ, Germany, catalog no.: Acc635), used for lentivirus production, were obtained from DSMZ and cultivated in Dulbecco's modified Eagle's medium (Biowest, catalog no.: L0104) supplemented with 10% fetal calf serum (Catus Biotech, catalog no.: BS- 2020-500). All OCI-AML (Luc⁺/GFP⁺) cell lines (DSMZ, Germany, catalog no.: ACC 582, ACC 99) were cultured in minimum essential medium α (PAN-Biotech, catalog no.: P04-21250) supplemented with 20% fetal calf serum.

Plasmid constructs

The second-generation CD33-CAR contained an My96 clone-derived scFv, linked via CD8-derived spacer and transmembrane domain (UniProt IDP01732, aa138-206) to a 4-1BB costimulatory domain (UniProt ID: Q07011, aa214-255) and a CD3 ζ signaling domain (RefSeq ID: NP_000725.1, aa52-163).²¹ The dNPM1-TCR sequence was identified and previously described by Van der Lee et al.¹⁹ CD33-CAR and dNPM1-TCR were cloned into a lentiviral plasmid backbone.

Manufacturing of T cells co-expressing CD33-CAR and dNPM1-TCR

Peripheral blood mononuclear cells were purified from healthy donor blood (University hospital Hagen or Dortmund, Germany) through density gradient centrifugation. Subsequently, magnetic enrichment of CD8⁺ or CD4⁺ T cells was performed using the CD8⁺ or CD4⁺ T cell isolation kit, human, respectively. Isolated T cells were cultured at a density of 1×10^6 /mL in TexMACS, supplemented with 12.5 ng/mL interleukin (IL)-7 and IL-15. TransAct was added in a dilution of 1:100 for activation at day of isolation. The next day, T cells were lentivirally transduced and 2 days post-transduction, the media was completely exchanged by TexMACS supplemented with 12.5 ng/mL IL-7 and IL-15 and 3% human AB serum (Capricorn Scientific, Ebsdorfergrund, Germany).

To ensure high comparability between CAR⁺TCR-T cells and the other controls for *in vitro* functionality testing, all effector cell types were enriched using MACSQuant Tyto. The cells were sorted using anti-CD8 antibody, anti-CD33-CAR detection reagent and/or dNPM1-TCR-specific Tetramer. After sorting, T cells were re-activated using TransAct in a dilution of 1:500 and then cultivated for 7 more days before co-culture assay.

Large-scale manufacturing of CD8⁺ effector T cells for *in vivo* analyses was performed using the fully closed and automated CliniMACS Prodigy platform (Miltenyi Biotec) with a leukapheresis from Biomex GmbH (Germany) as starting material and a transduction and cultivation process as previously described.⁴⁶

Functionality assays *in vitro*

Effector cells were co-cultured with GFP⁺ target cells at an E:T ratio and duration as indicated in the figure legends to assess the cytolytic activity. The cytotoxicity was performed in 96-well format with duplicates for each condition. Target cell count was determined at

MACSQuant Analyzer 10 or X (Miltenyi Biotec) and data was analyzed with FlowLogic V.8 software (Inivai Technologies). Long-term *in vitro* co-culture experiments with repeated addition of new target cells were analyzed using live-cell imaging system Incucyte S3 (Sartorius). The GFP intensities of OCI-AML target cells were determined as integrated values normalized to the starting time point. Cytokine concentrations in co-culture supernatants were determined after 18 h using MACSplex Cytokine Kit (catalog no.: 130-099-169).

Flow cytometry analysis

MACSQuant Analyzer 10 or X (Miltenyi Biotec) were used for flow cytometry analysis of the transduction efficiency, the target cell count after co-culture and the T cell exhaustion and differentiation phenotype. Cell staining was performed in CliniMACS PBS/EDTA Buffer supplemented with 0.5% bovine serum albumin. Staining with fluorescently labeled antibodies was performed protected from light at 4°C for 10 min. Tetramer staining was performed at room temperature and first step, prior to antibody staining. All antibodies were used according to manufacturer's instructions: Phenotype markers: CD45RO-APC-Vio 770/-APC (clone: REA611), CD62L-PE-Vio 770/-PE (clone: REA615), CD95-Pe-Vio 770 (clone: REA738); Exhaustion markers: CD223-APC-Vio 770 (clone: REA351), CD366-PE-Vio (clone: REA636); Transduction efficiency: dNPM1-specific PE-labeled Tetramer, CD33-CAR Alexa Fluor 647-conjugated detection reagent; *Ex vivo* staining: anti-mouse Ter-119-PerCP-Vio 770 (clone: REA847), CD4-VioBlue (clone: REA623), CD8-VioBlue-FITC (clone: REA734), CD33-APC (clone: REA775).

Bulk RNA sample preparation and sequencing

CD8⁺ CD33-CAR and/or dNPM1-TCR-expressing T cells were sorted directly via staining of CAR and/or TCR using MACSQuant Tyto. After re-activation with TransAct in a dilution of 1:500 and cultivation for 7 more days, co-culture with CD33⁺ dNPM1⁺ OCI-AML3 cells was performed for 18 h at an E:T ratio of 2:1. After magnetic depletion of target cells via CD4 and CD15, the effector cells were prepared for whole transcriptome analysis.

RNA was extracted using RNeasy Mini Kit (QIAGEN). RNA yield was quantified using Qubit RNA HS Assay kit (Thermo Fischer Scientific, catalog no.: Q32852) and quality was assessed with RNA 6000 Nano Chip (Agilent). Whole transcriptome libraries were generated using QIAseq Stranded mRNA kit (QIAGEN, catalog no.: 180450). The final libraries were quantified by Qubit dsDNA HS Assay kit (Thermo Fischer Scientific, catalog no.: Q32851), Bioanalyzer High sensitivity DNA Assay (Agilent, catalog no.: 5067-4626) and quantitative PCR with the NEB Next Library Quant Kit for Illumina (New England Biolabs, catalog no.: E7630L). Sequencing was performed on Illumina MiSeq as QC run, and finally on Illumina NextSeq 550.

Whole transcriptome analysis

Pre-processing of the data was done using CLC Genomics Workbench 23.0.2 (QIAGEN). Raw reads were trimmed and mapped to GRCh38 genome and to annotated transcripts from Ensembl v106. Mapped reads were assigned to the transcripts using the expectation

maximization estimation algorithm, and expression values for each gene were obtained by summing the transcript counts belonging to the gene. Quality control of the data was performed in CLC Genomics Workbench 23.0.2 (QIAGEN). Read count exceeded 40 million reads with least 87% mapping rate in all samples. Count matrix was loaded into RStudio using R for further analysis. Genes that were expressed in at least 20% of the samples with an average count per million higher than 1 (CPM >1) were considered minimally expressed and kept for downstream analyses. DESeq2 v.1.38.2 was used for model selection and differential gene expression.⁴⁷ Predictor importance of experimental variables was evaluated using a likelihood ratio test, setting an adjusted (Benjamini-Hochberg) *p* value < 0.05 as a cutoff. Effector cells and specific stimulus were included in the model. Hierarchical clustering (Euclidian distance, method “complete”) using pheatmap v.1.0.12⁴⁸ was performed on the 500 most variable genes (centered and scaled matrix), and we observed clustering mainly due to effector cell type. DEGs were determined setting an adjusted (Benjamini-Hochberg) *p* value < 0.05 as a cutoff. Gene set enrichment analysis was performed with topGO v2.46.0 using minimal node size of 10 and the elimination method to correct for structure dependency.²³ To facilitate interpretability, ReactomePA v1.38.0 was used to find enriched pathways.²⁵ For both analyses, false discovery rate correction was performed and enriched terms with an adjusted (Benjamini-Hochberg) *p* value < 0.05 were kept. Up- and downregulated genes were analyzed separately.

AML xenograft mouse model

Pre-clinical testing in mice was approved by the local ethics committee Landesamt für Natur, Umwelt und Verbraucherschutz Nordrhein-Westfalen (reference number: 81–02.04.2022.A412). The study was performed in accordance with German (TierSchG §§ 7–9 and TierSchVerV) and European (EU, Directive 2010/63/EU) guidelines. The efficacy study was performed with female, immunodeficient NOD.Cg-Prkdc^{scid} IL2rg^{tm1Wjl}/SzJ (NSG) mice (Charles River Laboratories, Wilmington, MA, USA). 1×10^6 OCI-AML3 (Luc⁺/tdTomato⁺) diluted in 100 μ L Gibco PBS (Thermo Fisher Scientific, catalog no.: 10010023) were intravenously injected via the tail vein. After randomization on day 3 and tumor engraftment for a total of 4 days, $5\text{--}7 \times 10^6$ engineered effector T cells diluted in 100 μ L CliniMACS Formulation was injected intravenously. More precisely, the transduction efficiency was normalized to approximately 60% through addition of untransduced cells, resulting in 7.9×10^6 total T cells per mouse. The *in vivo* imaging system Lumina III (IVIS, PerkinElmer) was used twice a week to determine whole-body luminescence (p/s) by intraperitoneally injecting 3 mg D-Luciferin (Gold Biotechnology, catalog no.: 115144-35-9) dissolved in 100 μ L PBS.

For *ex vivo* analysis, spleens were collected in RPMI medium and homogenized using program m_spleen_01_01 at gentleMACS Octo Dissociator (Miltenyi Biotec). The lysate was filtered through 70 μ m Pre-Separation filters, centrifuged at $300 \times g$ for 5 min and finally re-suspended in autoMACS Running Buffer for staining and flow-cytometric analysis.

Statistics

GraphPad Prism version 8.1.2. (GraphPad, USA) was used to perform data analysis. The type of test was chosen according to the experimental setup and is mentioned in the figure legends.

DATA AND CODE AVAILABILITY

The data presented in this study are available on request from the corresponding author.

SUPPLEMENTAL INFORMATION

Supplemental information can be found online at <https://doi.org/10.1016/j.omton.2024.200797>.

ACKNOWLEDGMENTS

The authors acknowledge the scientific advice of Mario Assenmacher, Pradyot Dash, Nicole Cordes, and Ian Johnson as well as the technical assistance of Shima Ferdos, Carolin Kolbe, and Nele Knelangen during *ex vivo* analysis. The authors also thank Dina Schneider for providing the CD33 CAR construct as well as Lilian Andrea Martinez-Carrera and Stefan Tomiuk for supporting the RNA-seq analysis. Furthermore, the authors acknowledge the support of Marvin Markel, Lennart Wessels, and Marek Wieczorek for the Tetramer production and Thorge Reiber for conjugating the CD33-CAR Detection Reagent.

AUTHOR CONTRIBUTIONS

K.T., A.K., and D.L. conceptualized the study; K.T., I.E.Y.O., C.B., V.H., N.Winter, and N.Werchau generated and analyzed data; I.E.Y.O., S.K., C.W., N.J., and K.V. generated and analyzed the RNA-seq data. B.E., T.S., and K.A. supervised defined aspects of the study; K.T. drafted the work; and A.K. and D.L. substantially revised the manuscript. All authors read and approved the submitted manuscript.

DECLARATION OF INTERESTS

K.T., I.E.Y.O., C.B., V.H., N.Winter, N.Werchau, S.K., C.W., N.J., K.B., B.E., T.S., and D.L. are employees of Miltenyi Biotec B.V. & Co. KG.

REFERENCES

- Zhang, X., Zhu, L., Zhang, H., Chen, S., and Xiao, Y. (2022). CAR-T Cell Therapy in Hematological Malignancies: Current Opportunities and Challenges. *Front. Immunol.* *13*, 927153.
- Marvin-Peek, J., Savani, B.N., Olalekan, O.O., and Dholaria, B. (2022). Challenges and Advances in Chimeric Antigen Receptor Therapy for Acute Myeloid Leukemia. *Cancers* *14*, 497.
- Pelcovits, A., and Niroula, R. (2020). Acute Myeloid Leukemia: A Review. *R. I. Med. J.* *103*, 38–40.
- Takami, A. (2018). Hematopoietic stem cell transplantation for acute myeloid leukemia. *Int. J. Hematol.* *107*, 513–518.
- Tettamanti, S., Pievani, A., Biondi, A., Dotti, G., and Serafini, M. (2022). Catch me if you can: how AML and its niche escape immunotherapy. *Leukemia* *36*, 13–22.
- Rotiroli, M.C., Buracchi, C., Arcangeli, S., Galimberti, S., Valsecchi, M.G., Perriello, V.M., Rasko, T., Alberti, G., Magnani, C.F., Cappuzzello, C., et al. (2020). Targeting CD33 in Chemoresistant AML Patient-Derived Xenografts by CAR-CIK Cells Modified with an Improved SB Transposon System. *Mol. Ther.* *28*, 1974–1986.

7. Atila, E., and Benabdellah, K. (2023). The Black Hole: CAR T Cell Therapy in AML 15.
8. Kenderian, S.S., Ruella, M., Shestova, O., Klichinsky, M., Aikawa, V., Morrissette, J.J.D., Scholler, J., Song, D., Porter, D.L., Carroll, M., et al. (2015). CD33-specific chimeric antigen receptor T cells exhibit potent preclinical activity against human acute myeloid leukemia. *Leukemia* 29, 1637–1647.
9. Sievers, E.L., Larson, R.A., Stadtmauer, E.A., Estey, E., Löwenberg, B., Dombret, H., Karanes, C., Theobald, M., Bennett, J.M., Sherman, M.L., et al. (2001). Efficacy and safety of gemtuzumab ozogamicin in patients with CD33-positive acute myeloid leukemia in first relapse. *J. Clin. Oncol.* 19, 3244–3254.
10. Sun, Y., Dong, Y., Sun, R., Liu, Y., Wang, Y., Luo, H., Shi, B., Jiang, H., and Li, Z. (2022). Chimeric anti-GPC3 sFv-CD3epsilon receptor-modified T cells with IL7 co-expression for the treatment of solid tumors. *Mol. Ther. Oncolytics* 25, 160–173.
11. Desai, R.H., Zandvakili, N., and Bohlander, S.K. (2022). Dissecting the Genetic and Non-Genetic Heterogeneity of Acute Myeloid Leukemia Using Next-Generation Sequencing and In Vivo Models. *Cancers* 14, 2182.
12. Molica, M., Perrone, S., Mazzone, C., Niscola, P., Cesini, L., Abruzzese, E., and de Fabritiis, P. (2021). CD33 Expression and Gemtuzumab Ozogamicin in Acute Myeloid Leukemia: Two Sides of the Same Coin. *Cancers* 13, 3214.
13. Liu, F., Cao, Y., Pinz, K., Ma, Y., Wada, M., Chen, K., Ma, G., Shen, J., Tse, C.O., Su, Y., et al. (2018). First-in-Human CLL1-CD33 Compound CAR T Cell Therapy Induces Complete Remission in Patients with Refractory Acute Myeloid Leukemia: Update on Phase 1 Clinical Trial. *Blood* 132, 901.
14. Limongello, R., Marra, A., Mancusi, A., Bonato, S., Hoxha, E., Ruggeri, L., Hui, S., Velardi, A., and Pierini, A. (2021). Novel Immune Cell-Based Therapies to Eradicate High-Risk Acute Myeloid Leukemia. *Front. Immunol.* 12, 695051.
15. Tambaro, F.P., Singh, H., Jones, E., Rytting, M., Mahadeo, K.M., Thompson, P., Daver, N., DiNardo, C., Kadia, T., Garcia-Manero, G., et al. (2021). Autologous CD33-CAR-T cells for treatment of relapsed/refractory acute myelogenous leukemia. *Leukemia* 35, 3282–3286.
16. Kang, S., Li, Y., Qiao, J., Meng, X., He, Z., Gao, X., and Yu, L. (2022). Antigen-Specific TCR-T Cells for Acute Myeloid Leukemia: State of the Art and Challenges. *Front. Oncol.* 12, 787108.
17. Xie, N., Shen, G., Gao, W., Huang, Z., Huang, C., and Fu, L. (2023). Neoantigens: promising targets for cancer therapy. *Signal Transduct. Target. Ther.* 8, 9.
18. Papaemmanuil, E., Gerstung, M., Bullinger, L., Gaidzik, V.I., Paschka, P., Roberts, N.D., Potter, N.E., Heuser, M., Thol, F., Bolli, N., et al. (2016). Genomic Classification and Prognosis in Acute Myeloid Leukemia. *N. Engl. J. Med.* 374, 2209–2221.
19. Van der Lee, D.I., Reijmers, R.M., Honders, M.W., Hagedoorn, R.S., de Jong, R.C., Kester, M.G., van der Steen, D.M., de Ru, A.H., Kweekeel, C., Bijen, H.M., et al. (2019). Mutated nucleophosmin 1 as immunotherapy target in acute myeloid leukemia. *J. Clin. Invest.* 129, 774–785.
20. Teppert, K., Wang, X., Anders, K., Evaristo, C., Lock, D., and Künkele, A. (2022). Joining Forces for Cancer Treatment: From "TCR versus CAR" to "TCR and CAR". *Int. J. Mol. Sci.* 23, 14563.
21. Schneider, D., Xiong, Y., Hu, P., Wu, D., Chen, W., Ying, T., Zhu, Z., Dimitrov, D.S., Dropulic, B., and Orentas, R.J. (2018). A Unique Human Immunoglobulin Heavy Chain Variable Domain-Only CD33 CAR for the Treatment of Acute Myeloid Leukemia. *Front. Oncol.* 8, 539.
22. Elias Yonezawa Ogusuku, I., Herbel, V., Lennartz, S., Brandes, C., Argiro, E., Fabian, C., Hauck, C., Hoogstraten, C., Veld, S., Hageman, L., et al. (2024). Automated manufacture of ΔNPM1 TCR-engineered T cells for AML therapy. *Mol. Ther. Methods Clin. Dev.* 32, 101224. <https://doi.org/10.1016/j.omto.2024.101224>.
23. Alexa, A., Rahnenführer, J., and Lengauer, T. (2006). Improved scoring of functional groups from gene expression data by decorrelating GO graph structure. *Bioinformatics* 22, 1600–1607.
24. Croft, D., O'Kelly, G., Wu, G., Haw, R., Gillespie, M., Matthews, L., Caudy, M., Garapati, P., Gopinath, G., Jassal, B., et al. (2011). Reactome: a database of reactions, pathways and biological processes. *Nucleic Acids Res.* 39, D691–D697.
25. Yu, G., and He, Q.-Y. (2016). ReactomePA: an R/Bioconductor package for reactome pathway analysis and visualization. *Mol. Biosyst.* 12, 477–479.
26. Saoudi, A., Kassem, S., Dejean, A., and Gaud, G. (2014). Rho-GTPases as key regulators of T lymphocyte biology. *Small GTPases* 5, e28208.
27. Krawczyk, C., and Penninger, J.M. (2001). Molecular motors involved in T cell receptor clusterings. *J. Leukoc. Biol.* 69, 317–330.
28. Chevallier, P., Delaunay, J., Turlure, P., Pigneux, A., Hunault, M., Garand, R., Guillaume, T., Avet-Loiseau, H., Dmytruk, N., Girault, S., et al. (2008). Long-Term Disease-Free Survival After Gemtuzumab, Intermediate-Dose Cytarabine, and Mitoxantrone in Patients With CD33+ Primary Resistant or Relapsed Acute Myeloid Leukemia. *J. Clin. Oncol.* 26, 5192–5197.
29. Qin, H., Yang, L., Chukinas, J.A., Shah, N., Tarun, S., Pouzolles, M., Chien, C.D., Niswander, L.M., Welch, A.R., Taylor, N., et al. (2021). Systematic preclinical evaluation of CD33-directed chimeric antigen receptor T cell immunotherapy for acute myeloid leukemia defines optimized construct design. *J. Immunother. Cancer* 9, e003149.
30. Shahzad, M., Nguyen, A., Hussain, A., Ammad-Ud-Din, M., Faisal, M.S., Tariq, E., Ali, F., Butt, A., Anwar, I., Chaudhary, S.G., et al. (2023). Outcomes with chimeric antigen receptor t-cell therapy in relapsed or refractory acute myeloid leukemia: a systematic review and meta-analysis. *Front. Immunol.* 14, 1152457.
31. Molon, B., Gri, G., Bettella, M., Gómez-Moutón, C., Lanzavecchia, A., Martínez-A, C., Mañes, S., and Viola, A. (2005). T cell costimulation by chemokine receptors. *Nat. Immunol.* 6, 465–471.
32. Felce, J.H., Parolini, L., Sezgin, E., Céspedes, P.F., Korobchevskaia, K., Jones, M., Peng, Y., Dong, T., Fritzsche, M., Aarts, D., et al. (2020). Single-Molecule, Super-Resolution, and Functional Analysis of G Protein-Coupled Receptor Behavior Within the T Cell Immunological Synapse. *Front. Cell Dev. Biol.* 8, 608484.
33. Wang, D. (2018). The essential role of G protein-coupled receptor (GPCR) signaling in regulating T cell immunity. *Immunopharmacol. Immunotoxicol.* 40, 187–192.
34. Ngai, J., Methi, T., Andressen, K.W., Levy, F.O., Torgersen, K.M., Vang, T., Wettschureck, N., and Taskén, K. (2008). The heterotrimeric G-protein alpha-subunit Galphaq regulates TCR-mediated immune responses through an Lck-dependent pathway. *Eur. J. Immunol.* 38, 3208–3218.
35. Chavez, M., Rane, D.A., Chen, X., and Qi, L.S. (2023). Stable expression of large transgenes via the knock-in of an integrase-deficient lentivirus. *Nat. Biomed. Eng.* 7, 661–671.
36. Ricobaraza, A., Gonzalez-Aparicio, M., Mora-Jimenez, L., Lumberras, S., and Hernandez-Alcoceba, R. (2020). High-Capacity Adenoviral Vectors: Expanding the Scope of Gene Therapy. *Int. J. Mol. Sci.* 21, 3643.
37. Pizzitola, I., Anjos-Afonso, F., Rouault-Pierre, K., Lassailly, F., Tettamanti, S., Spinelli, O., Biondi, A., Biagi, E., and Bonnet, D. (2014). Chimeric antigen receptors against CD33/CD123 antigens efficiently target primary acute myeloid leukemia cells in vivo. *Leukemia* 28, 1596–1605.
38. Kell, W.J., Burnett, A.K., Chopra, R., Yin, J.A.L., Clark, R.E., Rohatiner, A., Culligan, D., Hunter, A., Prentice, A.G., and Milligan, D.W. (2003). A feasibility study of simultaneous administration of gemtuzumab ozogamicin with intensive chemotherapy in induction and consolidation in younger patients with acute myeloid leukemia. *Blood* 102, 4277–4283.
39. Boucher, J.C., Shrestha, B., Vishwasrao, P., Leick, M., Cervantes, E.V., Ghafour, T., Reid, K., Spittler, K., Yu, B., Betts, B.C., et al. (2023). Bispecific CD33/CD123 targeted chimeric antigen receptor T cells for the treatment of acute myeloid leukemia. *Mol. Therapy - Oncolytics* 31. <https://doi.org/10.1016/j.omto.2023.100751>.
40. Wang, Y., Lu, W., Rohrbacher, L., Flaswinkel, H., Emhardt, A.J., Magno, G., Haubner, S., Kobold, S., Leonhardt, H., Hopfner, K.-P., et al. (2023). CD33-TIM3 Dual CAR T Cells: Enhancing Specificity While Maintaining Efficacy Against AML. *Blood* 142, 3449.
41. Zhang, R.-Y., Wei, D., Liu, Z.-K., Yong, Y.-L., Wei, W., Zhang, Z.-Y., Lv, J.-J., Zhang, Z., Chen, Z.-N., and Bian, H. (2019). Doxycycline Inducible Chimeric Antigen Receptor T Cells Targeting CD147 for Hepatocellular Carcinoma Therapy. *Front. Cell Dev. Biol.* 7, 233.
42. Kim, M.Y., Yu, K.R., Kenderian, S.S., Ruella, M., Chen, S., Shin, T.H., Aljanahi, A.A., Schreeder, D., Klichinsky, M., Shestova, O., et al. (2018). Genetic Inactivation of CD33 in Hematopoietic Stem Cells to Enable CAR T Cell Immunotherapy for Acute Myeloid Leukemia. *Cell* 173, 1439–1453.e19.
43. Liu, Y., Wang, S., Schubert, M.L., Lauk, A., Yao, H., Blank, M.F., Cui, C., Janssen, M., Schmidt, C., Göllner, S., et al. (2022). CD33-directed immunotherapy with

- third-generation chimeric antigen receptor T cells and gemtuzumab ozogamicin in intact and CD33-edited acute myeloid leukemia and hematopoietic stem and progenitor cells. *Int. J. Cancer* *150*, 1141–1155.
44. van der Lee, D.I., Koutsoumpli, G., Reijmers, R.M., Honders, M.W., de Jong, R.C.M., Remst, D.F.G., Wachsmann, T.L.A., Hagedoorn, R.S., Franken, K.L.M.C., Kester, M.G.D., et al. (2021). An HLA-A*11:01-Binding Neoantigen from Mutated NPM1 as Target for TCR Gene Therapy in AML. *Cancers* *13*, 5390.
45. Hassan, N., Yang, J., and Wang, J.Y. (2020). An Improved Protocol for Establishment of AML Patient-Derived Xenograft Models. *STAR Protoc.* *1*, 100156.
46. Lock, D., Mockel-Tenbrinck, N., Drechsel, K., Barth, C., Mauer, D., Schaser, T., Kolbe, C., Al Rawashdeh, W., Brauner, J., Hardt, O., et al. (2017). Automated Manufacturing of Potent CD20-Directed Chimeric Antigen Receptor T Cells for Clinical Use. *Hum. Gene Ther.* *28*, 914–925.
47. Love, M.I., Huber, W., and Anders, S. (2014). Moderated estimation of fold change and dispersion for RNA-seq data with DESeq2. *Genome Biol.* *15*, 550.
48. Kolde, R. (2019). pheatmap: Pretty Heatmaps Version 1.0.12. <https://cran.r-project.org/package=pheatmap>.